International Journal of Applied Mathematics

Volume 33 No. 4 2020, 599-608
ISSN: 1311-1728 (printed version); ISSN: 1314-8060 (on-line version)
doi: http://dx.doi.org/10.12732/ijam.v33i4.5

A GENERALIZED FINITE-DIFFERENCES SCHEME USED IN MODELING OF A DIRECT AND AN INVERSE PROBLEM OF ADVECTION-DIFFUSION

F. Domínguez-Mota[1 §], J.S. Lucas-Martínez[2], G. Tinoco-Guerrero[3]
[1,2,3] F.C.F.M, U.M.S.N.H
Francisco J. Mújica S/N
Morelia - 58030, MEXICO

Abstract: This work presents the use of a schemes in generalized finite-differences for the calculation of a numeric solution associated to a stationary, advection-diffusion problem, and the usage of such schemes in the study of an inverse problem related to this one, in which a non-linear, regularized least-squares adjustment is employed to determine certain coefficients involved in the problem.

AMS Subject Classification: 75N06, 65M50, 74S20
Key Words: generalized finite difference method; advection-diffusion problem; inverse problem

1. Introduction

Advection-diffusion problems arise naturally when analyzing interactions between physical processes with its effect on species or components, or on heat. The transport processes are relevant in almost all environmental systems, since heat or mass transport are common phenomena which can be found practically everywhere in the planet.

Two different types of transport processes can be distinguished: advection and diffusion (or dispersion). Advection can be understood in a narrower sense as a basic process of transport: a particle is purely shifted from one place to

Received: February 28, 2020

§Correspondence author

another by a flow field. Diffusion or dispersion processes arise when a difference in concentration is involved. There exist a natural tendency among all systems to equalize concentration gradients. If the species have the possibility to move from one place to another, there will be a net diffusive or dispersive flux from a location with high concentration to locations with lower concentrations. In each of these transport processes which can be found in nature, conservation principles must be present as well.

The present work was first motivated by the study made by Manju Agarwal and Abhinav Tandon [1] on mesoscale wind, where they used a finite-difference scheme to model a two-dimension steady state problem. In their model, these authors used a model for mesoscale wind components used by Dilley and Yen [3] and a large-scale wind model used by Lin and Hieldemann [6]. The purpose of this work is to present a solution to a two-dimension, stationary advection-diffusion problem using a generalized finite-difference scheme, then to use this numerical solution as a benchmark to propose different and less complex models for the mesoscale wind components. Two new models are proposed, and the results obtained using such models were quite similar to the ones shown in [3, 6].

2. A stationary problem for benchmark

Consider the 2D stationary, advection-diffusion problem

$$u\frac{\partial C}{\partial x} + v\frac{\partial C}{\partial y} = \frac{\partial}{\partial x}\left(A\frac{\partial C}{\partial x}\right) + \frac{\partial}{\partial y}\left(A\frac{\partial C}{\partial y}\right), \tag{1}$$

defined over the domain $\Omega = [0,1] \times [0,1]$, with the parameters $u = v = 0.1$, $A(y) = 1+e^{-10y}$ and the boundary conditions $C(0,y) = C(1,y) = 0.05$, $\frac{\partial C}{\partial n} = 0$ in $[0,1] \times \{1\}$ and $\frac{\partial C}{\partial n} = g(x)$ in $[0,1] \times \{0\}$, where

$$g(x) = \begin{cases} 0.5 & \frac{3}{8} \leq x \leq \frac{5}{8}, \\ 0 & \text{otherwise.} \end{cases}$$

Our first step is to propose a generalized finite-differences scheme for this problem, which will then be used to study the inverse problem of interest. The mesh used to compute a numerical solution consist on a regular mesh in the domain, using 201 nodes on each direction, x and y, and then adding the diagonal going from the upper right corner to the lower left corner on each cell, which leads to a mesh similar as the one shown in Figure 1.

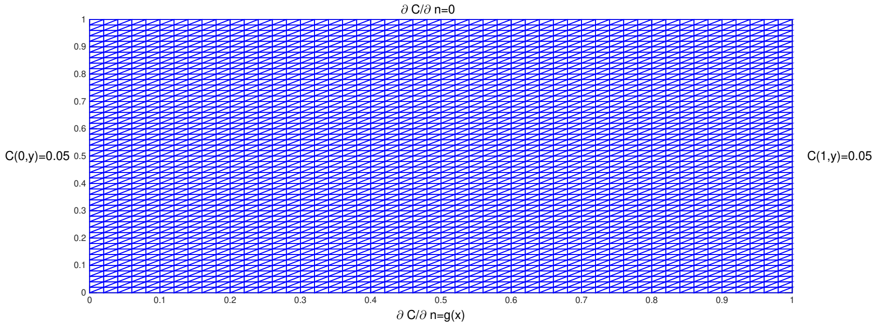

Figure 1: Mesh used in the computation of the numerical solution to (1), along with the boundary conditions for the problem.

In this mesh, each inner node has six neighbors, as shown in Figure 2. The goal is to find coefficients $\Gamma_0, \Gamma_1, ..., \Gamma_k$ such that the following consistency condition is fulfilled. Consider the second order linear operator:

$$L(\varphi, K_1(x,y), K_2(x,y), K_3(x,y), K_4(x,y), K_5(x,y)) =$$
$$K_1(x,y)\frac{\partial^2\varphi}{\partial x^2} + K_2(x,y)\frac{\partial^2\varphi}{\partial y^2} + K_3(x,y)\frac{\partial\varphi}{\partial x} + K_4(x,y)\frac{\partial\varphi}{\partial y} + K_5(x,y)\varphi.$$

This operator evaluated at the grid point $p_0 = (x_0, y_0)$ leads to the combination

$$L_0 := \sum_{l=1}^{6} \Gamma_l(p_0, p_l, K_1(x_0,y_0), K_2(x_0,y_0),$$
$$K_3(x_0,y_0), K_4(x_0,y_0), K_5(x_0,y_0))C(p_l),$$

which must satisfy the consistency condition

$$\tau(p_0) := [L(C, K_1(x,y), K_2(x,y), K_3(x,y),$$
$$K_4(x,y), K_5(x,y))]_{(x_0,y_0)} - L_0 \to 0,$$

as $p_1, ...p_6 \to p_0$, according to [2].

For the sake of brevity, let

$$\Gamma_l := \Gamma_l(p_0, p_l, K_1(x_l,y_l), K_2(x_l,y_l),$$
$$K_3(x_l,y_l), K_4(x_l,y_l), K_5(x_l,y_l)).$$

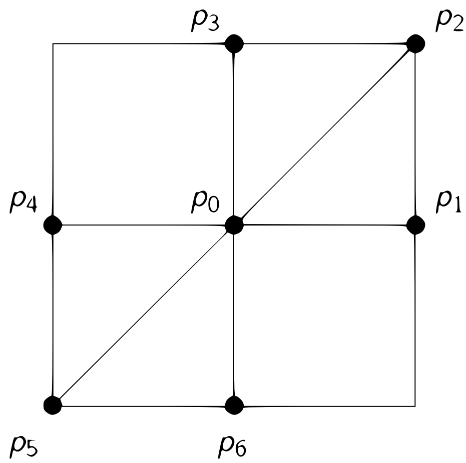

Figure 2: Neighbors distribution for an inner node in the mesh (1).

Let Δx_l and Δy_l be the x and y components of $p_l - p_0$, respectively.

Thus, the local truncation error $\tau(p_0)$ (up to second order) yields

$$\begin{aligned}
\tau(p_0) = & \left(K_5(x_0, y_0) - \sum_{i=0}^{6} \Gamma_i \right) C(p_0) + \left(K_3(x_0, y_0) - \sum_{i=1}^{6} \Gamma_i \Delta x_i \right) \frac{\partial C}{\partial x}(p_0) \\
& + \left(K_4(x_0, y_0) - \sum_{i=1}^{6} \Gamma_i \Delta y_i \right) \frac{\partial C}{\partial y}(p_0) \\
& + \left(K_1(x_0, y_0) - \sum_{i=1}^{6} \frac{\Gamma_i (\Delta x_i)^2}{2} \right) \frac{\partial^2 C}{\partial x^2}(p_0) \\
& + \left(- \sum_{i=1}^{6} \Gamma_i \Delta x_i \Delta y_i \right) \frac{\partial^2 C}{\partial x \partial y}(p_0) \\
& + \left(K_2(x_0, y_0) - \sum_{i=1}^{6} \frac{\Gamma_i (\Delta y_i)^2}{2} \right) \frac{\partial^2 C}{\partial y^2}(p_0) \\
& + \mathcal{O} \left(\max\{\Delta x_i, \Delta y_i\} \right)^3 .
\end{aligned}$$

If the function C from (1) is C^k for $k \geq 2$ [1], the previous equations can be

[1] It is to say, the first k derivatives exist and are continuous.

written as a system of linear equations

$$\begin{pmatrix} 1 & 1 & \dots & 1 \\ 0 & \Delta x_1 & \dots & \Delta x_6 \\ 0 & \Delta y_1 & \dots & \Delta y_6 \\ 0 & (\Delta x_1)^2 & \dots & (\Delta x_6)^2 \\ 0 & \Delta x_1 \Delta y_1 & \dots & \Delta x_6 \Delta y_6 \\ 0 & (\Delta y_1)^2 & \dots & (\Delta y_6)^2 \end{pmatrix} \begin{pmatrix} \Gamma_0 \\ \Gamma_1 \\ \Gamma_2 \\ \cdot \\ \cdot \\ \cdot \\ \Gamma_6 \end{pmatrix} = \begin{pmatrix} K_5(x_0, y_0) \\ K_3(x_0, y_0) \\ K_4(x_0, y_0) \\ 2K_1(x_0, y_0) \\ 0 \\ 2K_2(x_0, y_0) \end{pmatrix}. \tag{2}$$

It is worth to remark that this system of linear equations is not well-determined in general. In order to solve the system (2), the column of zeros and the row of ones can be put aside for a moment to solve the remaining system, and Γ_0 can be determined by the first equation of (2)

$$\sum_{i=0}^{6} \Gamma_i = K_5(x_0, y_0).$$

Adapting this system to problem (1), the remaining system can be written as

$$M\Gamma = \beta, \tag{3}$$

according to the node distribution shown in Figure 2, from which it is clear that $\Delta_x = \Delta_y := \Delta$:

$$M = \begin{pmatrix} \Delta & \Delta & 0 & -\Delta & -\Delta & 0 \\ 0 & \Delta & \Delta & 0 & -\Delta & -\Delta \\ \Delta^2 & \Delta^2 & 0 & \Delta^2 & \Delta^2 & 0 \\ 0 & \Delta^2 & 0 & 0 & \Delta^2 & 0 \\ 0 & \Delta^2 & \Delta^2 & 0 & \Delta^2 & \Delta^2 \end{pmatrix},$$

$$\Gamma = \begin{pmatrix} \Gamma_1 \\ \Gamma_2 \\ \cdot \\ \cdot \\ \cdot \\ \Gamma_6 \end{pmatrix}, \quad \beta = \begin{pmatrix} -u(x_0, y_0) \\ \frac{\partial A}{\partial y}(x_0, y_0) - v(x_0, y_0) \\ 2A(x_0, y_0) \\ 0 \\ 2A(x_0, y_0) \end{pmatrix}.$$

The previous system was solved using the pseudo inverse matrix, which led to the following numerical solution.

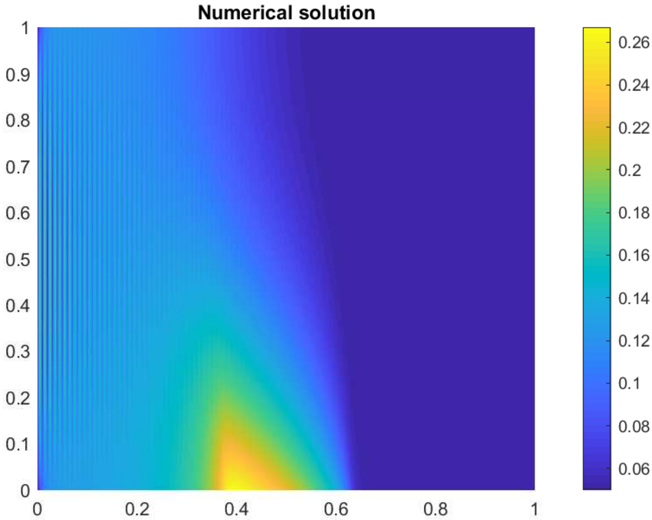

Figure 3: Numerical solution obtained for the problem (1).

3. The inverse problem

In the context of this work, by *inverse problem* it will be referred the following issue: given the numerical solution obtained for problem (1) in the previous section, suppose that such solution corresponds to an actual measurement of the concentration of a substance suspended in the atmosphere. The inverse problem discussed in this work is about determine some of the physical parameters involved in this advection-diffusion problem starting from the already-known solution; particularly, it will be about determine the parameters u and v from (1), which corresponds to the transport velocities. For the model of these parameters, Dilley and Yen [3] proposed the following functions, given as power laws:

$$u(x,y) = (U_1 - ax)\left(\frac{y}{y_1}\right)^m, \qquad v(y) = \frac{ay}{m+1}\left(\frac{y}{y_1}\right)^m,$$

where U_1, a, y_1, m are parameters to be determined, which are closely related to the physics involved in the problem.

The purpose of this work is to propose different functions to model the transport velocities u and v from (1), which could be used to replicate the solution already known. On the other hand, it would be desired for such functions

A_1	413.86	A_2	41.38
B_1	0.03	B_2	0.03
α_1	413.86	α_2	0.03

Table 1: Values found for the parameters in (4).

to be less complex that the ones proposed in [3]. The fist approach proposed is given by the following power laws:

$$u(x) = A_1 x^{\alpha_1} + B_1, \qquad v(y) = A_2 y^{\alpha_2} + B_2, \tag{4}$$

where the coefficients $A_1, A_2, B_1, B_2, \alpha_1, \alpha_2$ are constants to be determined. In comparison with the models proposed in [3], each of these approaches depends only of one space component, x and y respectively. The calculation of the parameters was made using the data from the numerical solution obtained in the previous section in a non-linear, regularized least-squares adjustment using the trust-region-reflective algorithm. The values found for such parameters are shown in Table 1.

The functions proposed in (4), along with the parameters just found, were used to compute a numerical solution to the problem (1) using the scheme in generalized finite-differences described in the previous section. Both numerical solutions are compared below.

As it can be seen in Figure 4, both numerical solutions are quite similar, which can be confirmed by the norm of the difference between these two matrices. The $||\cdot||_\infty$-norm of this difference is 1.608×10^{-10}, while the $||\cdot||_2$-norm of this difference is 4.6×10^{-9}.

The second model proposed is given as rational functions as follows:

$$u(x) = \frac{A_1 x + A_2}{A_3 x + A_4}, \qquad v(y) = \frac{B_1 y + B_2}{B_3 y + B_4}, \tag{5}$$

where the coefficients A_1, A_2, A_3, A_4 and B_1, B_2, B_3, B_4 are constants to be determined. Just like the model (4), each of these functions depends only on one space coordinate, x and y respectively. Here again, a non-linear, regularized least-squares adjustment using the data from the solution obtained in the previous section was used to determine the parameters required. The trust-region-reflective algorithm was also used. The values found for each parameter are shown below:

The numerical solution to (1) was calculated again replacing the functions u and v with the parameters just computed, using the same finite-differences

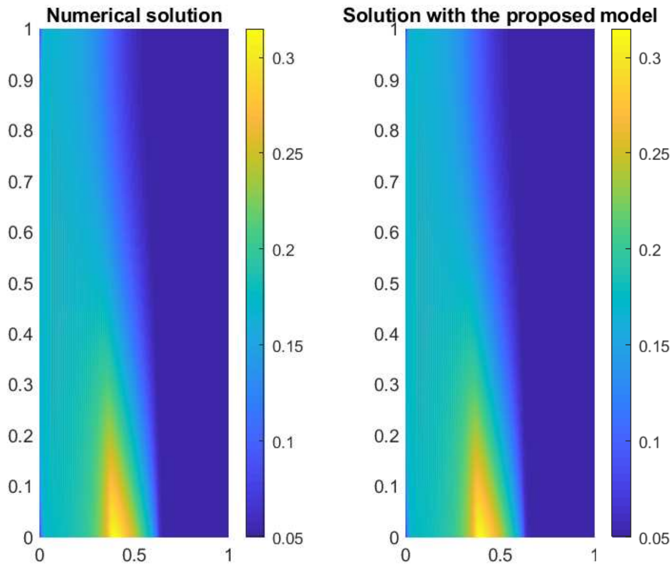

Figure 4: Comparison of both numerical solutions, using the exponential model (4).

scheme described in the previous section. The comparison between both numerical solutions is shown below. For comparison purposes, the norm of the difference between these two matrices was computed again. The $|| \cdot ||_\infty$-norm of this difference is 6.57×10^{-11}, while the $|| \cdot ||_2$-norm of this difference is 3.21×10^{-9}.

4. Conclusions

The generalized finite-difference scheme presented in section two provided a good approximation to get a numerical solution to the problem (1), despite the boundary conditions of the problem. Such scheme varies slightly from a scheme in classical finite-differences, but the addition of two extra nodes to each inner node in the grid allowed us the get a decent numerical solution. It can be seen in Figure 3 that the effects of the ill-posedness of the problem are still present, but such effects are due to the formulation of the problem instead of the scheme used to compute the solution.

A_1	0.0499	B_1	0.0501
A_2	0.0499	B_2	0.0501
A_3	0.0501	B_3	0.0499
A_4	0.0501	B_4	0.0499

Table 2: Values found for the parameters in (5).

Regarding section three, we would like to remark that it is possible to model the transport velocities involved in the formulation of problem (1) in a simpler way that the one presented in [3]. It must be recognized that the formulation made in [3] is much more related to the physics involved in the problem, but our claim is that a simpler approach for such parameters is also possible, which is a quite desirable feature when computing a numerical solution.

References

[1] M. Agarwal, A. Tandon. Modeling of the urban heat island in the form of mesoscale wind and of its effect on air pollution dispersal, *Applied Mathematical Modeling*, **34** (2010), 2520-2530.

[2] M. Celia, W. Gray, *Numerical Methods for Differential Equations*, Prentice-Hall (1992).

[3] J.F. Dilley, K.T. Yen, Effect of a mesoscale type wind on the pollutant distribution from a line source, *Atmos. Environ*, **6** (1971), 843-851.

[4] F.-J. Domínguez-Mota, S. Mendoza-Armenta, J.-G. Tinoco-Ruiz, G. Tinoco-Guerrero, Numerical solution of Poisson-like equations with Robin boundary conditions using a finite difference scheme defined by an optimality condition, In: *MASCOT11 Proceedings*, IMACS (2011), 101-110.

[5] H.W. Engl, *Inverse Problems*, Sociedad Matemática Mexicana (1995).

[6] J.S. Lin, L.M. Hieldemann, Analytical solution of the atmospheric diffusion equation with multiple sources and height dependent wind speed and eddy diffusivities, *Atmos. Environ.*, **30** (1996), 239-254.

[7] J.J.B. Muñoz, F. Ureña-Prieto, L. Corvinos, A. Gavete, Solving second order non-linear elliptic partial differential equations using generalized finite difference method, *J.of Comput. and Appl. Math.*, **318** (2017), 378-387.

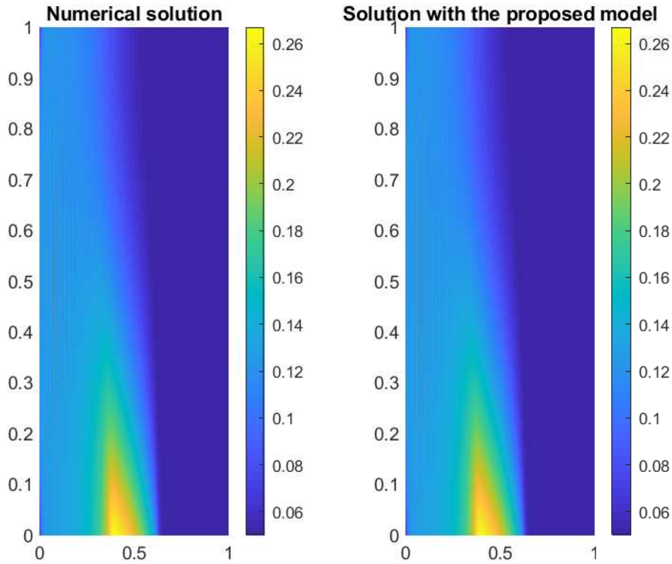

Figure 5: Comparison of both numerical solutions, using the rational model (5).

[8] J.J.B. Muñoz, F. Ureña-Prieto, L.A.G. Corvinos, Solving parabolic and hyperbolic equations by the generalized finite difference method, *J. of Comput. and Appl. Math.*, **209**, No 2 (2007), 208-233.

[9] J.J.B. Muñoz, F. Ureña-Prieto, L.A.G. Corvinos, Application of the generalized finite difference method to solve the advection diffusion equation, *J. of Comput. and Appl. Math.*, **2011** (2011), 1849-1855.

[10] G. Tinoco-Guerrero, F.J. Domínguez-Mota, A. Gaona-Arias, M.L. Ruiz-Zavala, J.G. Tinoco-Ruiz, A stability analysis for a generalized finite-difference scheme applied to the pure advection equation, *Mathematics and Computers in Simulation*, **147** (2018), 293-300.

[11] F. Ureña, J.J. Benito, L. Gavete, Application of the generalized finite difference method to solve the advection-diffusion equation, *J. of Comput. and Appl. Math.*, **235** (2011), 1849-1855.